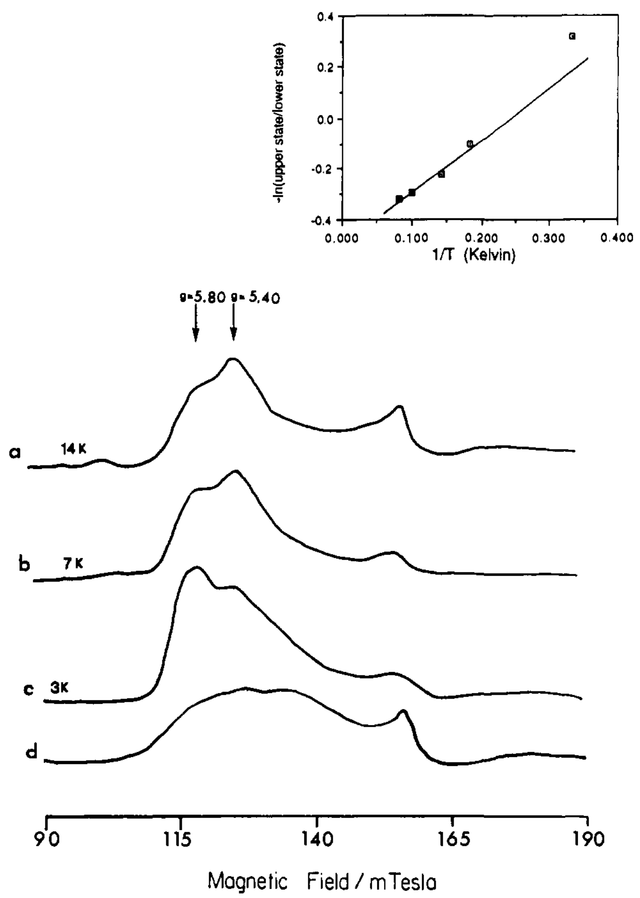

Figure 2. Effect of temperature and ethylene glycol on the $S = {}^{3}/_{2}$ spin signals of Av1′ spectrum. Buffer, protein concentration and specific activities as in Figure 1. Conditions: (a) temperature, 14 K; microwave power, 10 mW; modulation amplitude, 1 mT; frequency, 9.30 GHz; gain, 3.5×10^{6}; (b) temperature, 7 K; microwave power, 10 mW; modulation amplitude, 1 mT; frequency, 9.30 GHz; gain, 2.5×10^{6}; (c) temperature, 3 K; microwave power, 0.2 mW; modulation amplitude, 2 mT; frequency, 9.30 GHz; gain, 5×10^{5}; (d) conditions identical with those of figure (b) except solvent contains 50% ethylene glycol. Insert: plot of the negative natural logarithm of the ratio of the relative amplitudes of $g = 5.40$ to the $g = 5.80$ inflections versus the reciprocal of the absolute temperature. Inflection observed around 100 mT in (a) is not consistently observed in the Av1′ spectrum and, therefore, probably is exogenous to the Av1′ paramagnetism.

With use of $\lambda = 0.26$ and $g_0 = 2.06$ in eq 1 for Av1′, the predicted g' values are $g_{1x}' = 2.46$, $g_{1y}' = 5.40$, $g_{1z}' = 1.69$ for the first level and $g_{2x}' = 1.66$ and $g_{2y}' = 1.29$, $g_{2z}' = 5.80$ for the second. Obviously, the observed 5.80 and 5.40 inflections of Av1′ correspond to g_{2z}' and g_{1y}', respectively, while the remaining four inflections are undetectable, possibly due to g strain broadening.[12,13]

Since the two low field inflections represent different energy levels of the same $S = {}^{3}/_{2}$ spin system, their relative amplitudes must be coupled and temperature dependent. Figure 2 shows the low field region of Av1′ recorded at different temperatures, clearly demonstrating the temperature dependence of the shape of the spectrum and indicating that the intensity of the 5.8 signal increases with decreasing temperature and, therefore, implying that this signal corresponds to the ground-state level. For this inflection to correspond to the ground state, the axial zero-field splitting parameter, D, must be negative (as compared to a positive D for Av1). Furthermore, by plotting the natural logarithm of the ratio of the amplitudes of the two low field inflections against the reciprocal of the absolute temperature (insert in Figure 2), the magnitude of D can be calculated to be $-0.74\ \text{cm}^{-1}$. This value obviously is much smaller than that determined[6,7] for the Av1 ($\approx 6\ \text{cm}^{-1}$) and is consistent with the greater nesting observed in the magnetization of this paramagnetic cluster in Av1′ compared to that in Av1 as determined by MCD spectroscopy.[6]

Since the results recently reported on the MCD spectrum and magnetization of Av1′ were performed with the protein in a 50% ethylene glycol glass, it is important to determine whether this medium significantly perturbs the environment of the paramagnetic cluster. Figure 2d shows the spectrum of Av1′ recorded in 25 mM Tris·HCl buffer, pH 7.4, with 50% ethylene glycol. In the presence of ethylene glycol, the two low field inflections corresponding to the $S = {}^{3}/_{2}$ spin system are both significantly broadened and slightly shifted to higher fields. Due to this extensive broadening, no obvious g' values can be extracted from the spectrum. Spin integration[14] shows a slight increase in intensity of the $S = {}^{3}/_{2}$ system in the presence of ethylene glycol (0.94 spins per V atom in 50% ethylene glycol versus 0.89 spins per V atom in buffer), although the uncertainty in these integrations, especially in the presence of ethylene glycol where specific g' values are difficult to assign, may make this difference insignificant. Within experimental error, no significant change was observed in the integrated intensity of the axial $S = {}^{1}/_{2}$ signal at 2.04 and 1.93 in the two media.

In summary, the VFe protein of alternative nitrogenase, like the MoFe protein of the conventional nitrogenase, possesses a paramagnetism, part of which can be attributed to an $S = {}^{3}/_{2}$ spin system. The major differences between the two proteins is, first of all, the presence of an $S = {}^{1}/_{2}$ axial signal possibly associated with a reduced Fe–S cluster in Av1′ and, secondly, the much higher rhombicity and smaller (as well as negative) axial zero-field splitting parameter in the $S = {}^{3}/_{2}$ signal of the VFe protein. At present, it is not known whether these latter differences arise from the substitution of V for Mo in FeMo-co, differences in the proteins holding these cofactors or the production of an entirely new type of cofactor in FeV-co.

Acknowledgment. This work was supported by the National Institutes of Health under Grant GM 33965 and by Biomedical Shared Instrumentation Grant RR02838. We thank Ellen E. Case for help in the purification of these proteins.

---

(12) Hagen, W. R.; Hearshen, D. O.; Sands, R. H.; Dunham, W. R. *J. Magn. Reson.* **1985**, *61*, 220–232.

(13) Hagen, W. R.; Hearshen, D. O.; Harding, L. J.; Dunham, W. R. *J. Magn. Reson.* **1985**, *61*, 233–244.

(14) Aasa, R.; Vänngård, T. *J. Magn. Reson.* **1975**, *19*, 308–315.

Exceptional Efficacy of Some New Lacunar Dioxygen Carriers Based on Schiff Bases Derived from β-Diketones and Triamines

Rita Delgado, Mark W. Glogowski, and Daryle H. Busch*

Chemistry Department, The Ohio State University
Columbus, Ohio 43210

Received March 30, 1987

Dioxygen carriers continue to attract intense interest because of their immense promise in the many applications dependent on gas-phase dioxygen separations and because of the need to understand a variety of O_2 adducts in living systems.[1-4] The *performance parameters* and structure-parameter relationships that determine the efficacy of O_2 carriers are not thoroughly understood, but the greatest difficulties are associated with the fact that all dioxygen carriers are oxidized by O_2. The design of more efficacious oxygen carriers is a fascinating challenge.

---

(1) Busch, D. H. *Critical Care Medicine* **1982**, *10*, No. 4, 246.

(2) Bonaventura, J.; Bonaventura, C. U.S. Patent 4343815; August 10, 1982.

(3) Roman, I. U.S. Patent Application 393711, June 30, 1982.

(4) Adduci, A. J. *Chemtech* **1976**, 575.

Table I. Equilibrium Data for Cobalt Dioxygen Complexes

cobalt(II) complex	K_{O_2}, Torr^{-1}	temp, K
[Co{Me$_2$("C$_6$")Me$_2$malMeDPT}][a]	6.0 ± 0.2	263
	1.66 ± 0.05	273
	1.07 ± 0.08	278
	0.68 ± 0.04	283
	0.39 ± 0.01	288
	0.15 ± 0.02	298
[Co{Me$_2$("*p*-xylylene")-Me$_2$malMeDPT}][a]	$5.9 \pm 0.3 \times 10^{-2}$	253
	$2.71 \pm 0.04 \times 10^{-2}$	263
	$9.3 \pm 0.2 \times 10^{-3}$	273
	$6.7 \pm 0.3 \times 10^{-3}$	278
	$4.7 \pm 0.3 \times 10^{-3}$	283
	$1.1 \pm 0.2 \times 10^{-3}$	298
	ΔH (kJ/mol)[b]	ΔS (J/K mol)[b]
[Co{Me$_2$("C$_6$")Me$_2$malMeDPT}]	−68	−243
[Co{Me$_2$("*p*-xylylene")Me$_2$malMeDPT}]	−55	−239

[a] In toluene. [b] Standard state, 1 Torr.

The new lacunar pentadentate Schiff base complexes reported here (structures I and II) enjoy elements of completeness in molecular design that are not common among dioxygen carriers. All of the donor groups needed by the deoxy form of the metal ion are provided by the Schiff base which also provides a protected cavity for O_2 binding. Further, electron-withdrawing substituents protect against ligand oxidation.

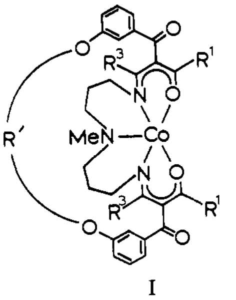

I

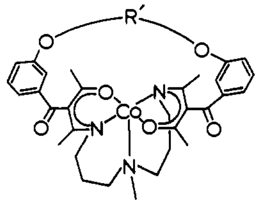

II

Exceptionally large O_2 affinities (Table I, K_{O_2}, Torr^{-1}) and a great resistance toward autoxidation mark these new complexes as unusually promising dioxygen carriers. The equilibrium constants for O_2 binding (measured as reported earlier[5,6]) for the optimal hexamethylene bridged complex are extraordinarily high for Schiff base complexes of cobalt(II).[7,8] The temperature dependence of K_{O_2} shows that the high O_2 affinities arise from the entropy term,[7,8] which may reflect decreased solvation of the oxygenated forms. Spectral scans showed complete reversibility over the temperature range from 253 to 298 K, as expected in view of preliminary results which show an autoxidation half-life for the hexamethylene derivative of 37 min at 50 °C in toluene solution at 197 Torr of O_2.

This new family of dioxygen carriers provides the opportunity to control performance parameters with structural variables over a wide range of dioxygen affinities but with similar good resistance to autoxidation. The *p*-xylylene bridged pentadentate complex shows a greatly reduced O_2 affinity (150–200×) when compared to the $(CH_2)_6$ bridged species (Table I). The values of ΔS are essentially identical for the two complexes with ΔH accounting for the control of O_2 affinity.[5,9,10]

The significance of the various structural features has been shown by counter examples. (1) **Effect of the lacuna**: The nonlacunar pentadentate complex of structure III gave evidence for formation of both the μ-peroxo dimer and the 1:1 O_2 complex; autoxidation is much more rapid than that of its lacunar counterpart. (2) **Effect of the built-in fifth donor**: Tetradentate cobalt(III) Schiff base complexes of structure IV[11] form both the μ-peroxo dimer and the 1:1 O_2 adduct, even in the presence of large excesses of axial ligands. Otherwise their properties are like those of the optimal pentadentate complex. (3) **Effect of the acyl substituents**: When R^2 in structure IV is a simple alkyl linkage[12] (decamethylene), the resulting lacunar complex autoxidizes at −10 °C in pyridine/toluene with a half-life of 200 s. Earlier studies have shown that the acyl substituent protects against oxidation of both the cobalt and the ligand,[13] thereby favoring reversible oxygen binding.[14]

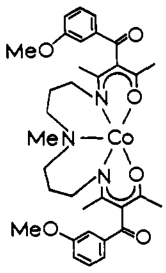

III

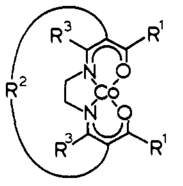

IV

The optimal complexes I were prepared from the copper(II)[11] complex of structure V.[15] The bridge design[11,16] (structure VI) has several highly favorable features. The benzoyl groups facilitate synthesis and lift the bridge above the coordination plane, providing a cavity or lacuna. The ether oxygen atoms provide critical flexibility. The meta position minimizes the electron-donating effect of the alkoxy unit both helping synthesis and contributing to autoxidative resistance. Variations in the link R′ control the size and shape of the cavity and, thereby, the O_2 affinity. The copper was removed as the sulfide, and the free ligand was characterized by its ^{13}C NMR, infrared, and mass spectra. The cobalt complex was formed by reaction between tetraethylammonium tetrabromocobaltate(II) and the ligand in dry *tert*-butyl alcohol in the presence of potassium *tert*-butoxide,[17] followed by concentrating the solution; the product was recrystallized from benzene/cyclohexane: yield, 55%. Anal. Calcd for $CoC_{37}N_3O_6H_{47}$: C, 64.53; H, 6.88; N, 6.10. Found: C, 64.75; H, 7.01; N, 6.00.

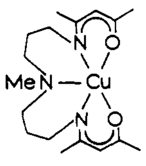

V

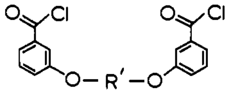

VI

The ESR spectra of the O_2 adducts indicate axial symmetry, like the parent tetradentate Schiff base complexes,[18] and contrast

---

[5] Stevens, J. C.; Busch, D. H. *J. Am. Chem. Soc.* **1980**, *102*, 3285.

[6] Herron, N.; Zimmer, L. L.; Grzybowski, J. J.; Olszanski, D. J.; Jackels, S. C.; Callahan, R. W.; Cameron, J. H.; Christoph, G. G.; Busch, D. H. *J. Am. Chem. Soc.* **1983**, *105*, 6585.

[7] Niederhoffer, E. C.; Timmons, J. H.; Martell, A. E. *Chem. Rev.* **1984**, *84*, 137.

[8] Carter, M. J.; Rillema, D. P.; Basolo. F. *J. Am. Chem. Soc.* **1974**, *96*, 392.

[9] Stevens, J. C. Ph.D. Thesis, The Ohio State University, 1979. Jackson, P. J. PhD. Thesis, The Ohio State University, 1981.

[10] Cameron, J. H.; Kojima, M.; Korybut-Daszkiewicz, B.; Coltrain, B. K.; Meade, T. J.; Alcock, N. W.; Busch, D. H. *Inorg. Chem.* **1987**, *26*, 427.

[11] Ramprasad, D.; Lin, W.-K.; Goldsby, K. A.; Busch, D. H., submitted for publication. Ramprasad, D.; Stephenson, N. A.; Busch, D. H., unpublished results.

[12] Minahan, D. M. A.; Stephenson, N. A.; Busch, D. H., unpublished results.

[13] Goldsby, K. A.; Jircitano, A. J.; Minahan, D. M.; Ramprasad, D.; Busch, D. H. *Inorg. Chem.* **1987**, *26*, 2651.

[14] Kubokura, K.; Okawa, H.; Kida, S. *Bull. Chem. Soc. Jpn.* **1978**, *51*, 2036.

[15] Braydich, M. D.; Fortman, J. J.; Cummings, S. C. *Inorg. Chem.* **1983**, *22*, 484.

[16] We thank Dr. Dorai Ramprasad for his help in extending the chemistry of the bridging reagent to these systems.

[17] Everett, G. W., Jr.; Holm, R. H. *J. Am. Chem. Soc.* **1965**, *87*, 2117.

[18] Hoffman, B. M.; Diemente, D. L.; Basolo, F. *J. Am. Chem. Soc.* **1970**, *92*, 61.

to more closely related pentadentate derivatives[15,19] which give rhombic signals. ESR spectrum of hexamethylene derivative: $g_\perp$, 1.977; $g_\parallel$, 2.096; $a_\perp$, 15.0; $a_\parallel$, 20.5 G. The value of $a_\parallel$ is consistent with the large dioxygen affinity.[15,19-21]

---

(19) Niswander, R. H.; Taylor, L. T. *J. Magn. Reson.* **1977**, *26*, 491.

(20) Niswander, R. H.; Taylor, L. T. *Inorg. Chem.* **1976**, *15*, 2360.

(21) We are grateful to the Calouste Gulbenkian Foundation (Lisbon, Portugal) for financial support.

A Priori Calculations of pK_a's for Organic Compounds in Water. The pK_a of Ethane

William L. Jorgensen,* James M. Briggs, and Jiali Gao

Department of Chemistry, Purdue University
West Lafayette, Indiana 47907

Received July 6, 1987

The enduring fascination of organic chemists with acidities and basicities reflects the fundamental importance of these concepts in understanding organic reactivity.[1] Developing scales of aqueous acidities for weak organic acids is challenging in view of the need for extrapolations from organic solvents to water, ion-pairing and aggregation effects for organometallic compounds, and the derivation of thermodynamic quantities from kinetic measurements.[1-4] The problems are reflected in the experimental ranges for the pK_a's of the simplest alkanes, methane and ethane, which cover from 40 to 60.[1a,e,3,4] In the present communication, we demonstrate how simulation methodology can be used to obtain a priori predictions for the relative pK_a's of organic compounds in water. The first applications are for the pK_a's of acetonitrile and ethane relative to methanethiol.

Consideration of the cycle below yields eq 1 where the aqueous

$$\begin{tikzcd}
\mathrm{AH} \arrow[r, "\Delta G_{\mathrm{gas}}"] \arrow[d, "\Delta G^{\mathrm{hyd}}(\mathrm{AH})"] & \mathrm{A}^- \arrow[d, "\Delta G^{\mathrm{hyd}}(\mathrm{A}^-)"] & + & \mathrm{H}^+ \arrow[d, "\Delta G^{\mathrm{hyd}}(\mathrm{H}^+)"] \\
\mathrm{AH} \arrow[r, "\Delta G_{\mathrm{aq}}"] & \mathrm{A}^- & + & \mathrm{H}^+
\end{tikzcd}$$

pK_a for AH is related to free energies of hydration and the gas-phase acidity. A similar expression for BH and subtraction provides eq 2 which shows that the difference in pK_a's has three

$$\Delta G_{\mathrm{aq}} = 2.3RT\,\mathrm{p}K_{\mathrm{a}}(\mathrm{AH}) = \Delta G^{\mathrm{hyd}}(\mathrm{A}^-) + \Delta G^{\mathrm{hyd}}(\mathrm{H}^+) - \Delta G^{\mathrm{hyd}}(\mathrm{AH}) + \Delta G_{\mathrm{gas}} \qquad (1)$$

$$2.3RT[\mathrm{p}K_{\mathrm{a}}(\mathrm{BH}) - \mathrm{p}K_{\mathrm{a}}(\mathrm{AH})] = \Delta\Delta G^{\mathrm{hyd}}(\mathrm{B}^- - \mathrm{A}^-) - \Delta\Delta G^{\mathrm{hyd}}(\mathrm{BH{-}AH}) + \Delta\Delta G_{\mathrm{gas}}(\mathrm{BH{-}AH}) \qquad (2)$$

components: the differences in free energies of hydration for the anions and for the neutrals and in the gas-phase acidities. These quantities can all be obtained with high precision by using modern theoretical methods, Monte Carlo or molecular dynamics simulations for the $\Delta\Delta G^{\mathrm{hyd}}$'s,[5-9] and ab initio quantum mechanics for $\Delta\Delta G_{\mathrm{gas}}$.[10-12]

Table I. Potential Function Parameters for the Anions

site	q (e^-)	σ (Å)	ϵ (kcal/mol)
		CH_3S^-	
C	−0.40	4.20	0.30
H	0.10	2.50	0.05
S	−0.90	4.25	0.50
		CH_2CN^-	
C1	−1.07	4.20	0.30
H	0.19	2.50	0.05
C2	0.51	3.65	0.15
N	−0.82	3.40	0.25
		$CH_3CH_2^-$	
C2	−0.40	4.20	0.30
H2	0.08	2.50	0.05
C1	0.00	4.20	0.30
H1	0.07	2.50	0.05
M[a]	−0.98	0.0	0.0

[a] M is a point in the plane of the HC1H bisector with r(C1–M) = 0.35 Å and ∠C2C1M = 117.75°

Table II. Computed and Experimental Free Energy Differences (kcal/mol) and pK_a's at 25 °C[a]

AH	$\Delta\Delta G^{\mathrm{hyd}}(\mathrm{A}^-)$	$\Delta\Delta G^{\mathrm{hyd}}(\mathrm{AH})$	$\Delta\Delta G_{\mathrm{gas}}$	pK_a
CH_3SH	0.0	0.0	0.0	(10.3)[b]
CH_3CN	5.2 ± 0.4	−1.3 ± 0.2	18.5	28.6 ± 0.3
	(4.3 ± 2)[c]	(−2.6)[c]	(11.7)[d]	(25 ± 1)[e]
CH_3CH_3	−6.4 ± 0.2	3.9 ± 0.1	65.3	50.6 ± 0.2
		(3.1)[c,f]	(60.8)[d,g]	(42–60)[h]

[a] Experimental values in parentheses. Error estimates for the computed values obtained as in ref 5. [b] Reference 1e. [c] Reference 17. [d] Reference 15. [e] Reference 24. [f] Reference 25. [g] Reference 16. [h] References 1a,e, 3, 4.

Briefly, the computations for the present three acids proceeded as follows. The ab initio calculations all employed the 6-31+G(d) basis set which includes d-orbitals and diffuse s- and p-orbitals on the non-hydrogen atoms.[13,14] Complete geometry optimizations were carried out for the three isolated anions and their conjugate acids, followed by calculations of the vibrational frequencies.[10] Correlation energies were computed with Møller–Plesset perturbation theory to third order, i.e., the calculations are denoted MP3/MP2/6-31+G(d)//6-31+G(d).[10] The ehthalpies, entropies, and free energies for ionization were then calculated in the usual way.[10,12] The results for $\Delta G^{298}_{\mathrm{gas}}$ are 349.2, 367.7, and 414.5 kcal/mol for CH_3SH, CH_3CN, and CH_3CH_3 which agree well with the experimental values 352.7,[15] 364.4,[15] and 413.5,[16] respectively,

---

(1) For reviews, see: (a) Cram, D. J. *Fundamentals of Carbanion Chemistry*; Academic Press: New York, 1965. (b) Bordwell, F. G. *Pure Appl. Chem.* **1977**, *49*, 963. (c) Streitwieser, A., Jr.; Juaristi, E.; Nebenzahl, L. L. In *Comprehensive Carbanion Chemistry, Part A*; Buncel, E., Durst, T., Eds.; Elsevier: Amsterdam, 1980; Chapter 7. (d) Taft, R. W. *Prog. Phys. Org. Chem.* **1983**, *14*, 247. (e) Stewart, R. *The Proton: Applications to Organic Chemistry*; Academic Press: New York, 1985. (f) Lowry, T. H.; Richardson, K. S. *Mechanism and Theory in Organic Chemistry*, 3rd ed.; Harper & Row: New York, 1987; Chapter 3.

(2) Streitwieser, A., Jr. *Acc. Chem. Res.* **1984**, *17*, 353.

(3) Juan, B.; Schwarz, J.; Breslow, R. *J. Am. Chem. Soc.* **1980**, *102*, 5741.

(4) Butin, K. P.; Beletskaya, I. P.; Kashin, A. N.; Reutov, O. A. *J. Organometal. Chem.* **1967**, *10*, 197.

(5) Jorgensen, W. L.; Ravimohan, C. *J. Chem. Phys.* **1985**, *83*, 3050.

(6) (a) Lybrand, T. P.; McCammon, J. A.; Wipff, G. *Proc. Natl. Acad. Sci. U.S.A.* **1986**, *83*, 833. (b) Wong, C. F.; McCammon, J. A. *J. Am Chem. Soc.* **1986**, *108*, 3830.

(7) Straatsma, T. P.; Berendsen, H. J. C.; Postma, J. P. M. *J. Chem. Phys.* **1986**, *85*, 6720.

(8) (a) Singh, U. C.; Brown, F. K.; Bash, P. A.; Kollman, P. A. *J. Am. Chem. Soc.* **1987**, *109*, 1607. (b) Bash, P. A.; Singh, U. C.; Langridge, R.; Kollman, P. A. *Science (Washington, D.C.)* **1987**, *236*, 564.

(9) Jorgensen, W. L.; Buckner, J. K.; Huston, S. E.; Rossky, P. J. *J. Am. Chem. Soc.* **1987**, *109*, 1891.

(10) Hehre, W. J.; Radom, L.; Schleyer, P. v. R.; Pople, J. A. *Ab Initio Molecular Orbital Theory*; Wiley: New York, 1986.

(11) Chandrasekhar, J.; Andrade, J. G.; Schleyer, P. v. R. *J. Am. Chem. Soc.* **1981**, *103*, 5609, 5612.

(12) Gao, J.; Garner, D. S.; Jorgensen, W. L. *J. Am. Chem. Soc.* **1986**, *108*, 4784.

(13) Binkley, J. S.; Whiteside, R. A.; Raghavachari, K.; Seeger, R.; DeFrees, D. J.; Schlegel, H. B.; Frisch, M J.; Pople, J. A.; Kahn, L. R. GAUSSIAN 82 *Release H*; Carnegie-Mellon University: Pittsburgh, 1982.

(14) Clark, T.; Chandrasekhar, J.; Spitznagel, G. W.; Schleyer, P. v. R. *J. Comput. Chem.* **1983**, *4*, 294.

(15) Bartmess, J. E.; McIver, R. T., Jr. In *Gas Phase Ion Chemistry, Volume 2*; Bowers, M. T.; Ed.; Academic Press: New York, 1979; p 87.

(16) DePuy, C. H.; Bierbaum, V. M.; Damrauer, R. *J. Am. Chem. Soc.* **1984**, *106*, 4051. The reported $\Delta H^\circ_{\mathrm{acid}}$ was converted to $\Delta G^{298}_{\mathrm{gas}}$ by subtracting 7.5 kcal/mol.[17] These values are somewhat ambiguous since the ethyl anion is unbound in the gas phase. See also: Schleyer, P. v. R.; Spitznagel, G. W.; Chandrasekhar, J. *Tetrahedron Lett.* **1986**, *27*, 4411.

0002-7863/87/1509-6857$01.50/0